

QCD sum rules for the anticharmed pentaquarkYasemin Sarac,^{1,*} Hungchong Kim,^{2,†} and Su Houn Lee^{3,‡}¹*Physics Department, Middle East Technical University, 06531 Ankara, Turkey*²*Department of Physics, Pohang University of Science and Technology, Pohang 790-784, Korea*³*Institute of Physics and Applied Physics, Yonsei University, Seoul 120-749, Korea*

(Received 25 October 2005; published 17 January 2006)

We present a QCD sum rule analysis for the anticharmed pentaquark state with and without strangeness. While the sum rules for most of the currents are either nonconvergent or dominated by the DN continuum, the one for the nonstrange pentaquark current composed of two diquarks and an antiquark is convergent and has a structure consistent with a positive-parity pentaquark state after subtracting out the DN continuum contribution. Arguments are presented on the similarity between the result of the present analysis and that based on the constituent quark models, which predict a more stable pentaquark state when the antiquark is heavy.

DOI: [10.1103/PhysRevD.73.014009](https://doi.org/10.1103/PhysRevD.73.014009)

PACS numbers: 14.20.Lq, 11.55.Hx, 12.38.Lg, 14.80.-j

I. INTRODUCTION

The observation of the Θ^+ by the LEPS Collaboration [1] and its subsequent confirmation have brought a lot of excitement to the field of hadronic physics [2]. On the other hand, there are an increasing number of experiments reporting negative results. In particular, the latest experiments at JLAB [3] find no signal from the photoproduction process on a deuteron nor on a proton target, from which the Θ^+ was observed earlier by the SAPHIR Collaboration with lower statistics. Although the present experimental results are quite confusing and frustrating [4], one cannot afford to give up further refined experimental search, because if a pentaquark is found, it will provide a major and unique testing ground for QCD dynamics at low energy.

Other multiplets to search for a possible pentaquark states are those with one heavy antiquark. The H1 Collaboration at HERA has recently reported on the findings of an anticharmed pentaquark $\Theta_c(3099)$ from the D^*p invariance mass spectrum [5]. Unfortunately other experiments could not confirm the finding [6–8]. While the experimental search for the heavy pentaquark is as confusing as that for the light, theoretically, the heavy and light pentaquarks stand on quite different grounds. Cohen showed that the original prediction for the mass of the Θ^+ based on the SU(3) Skyrme model [9] is not valid because collective quantization of the model for the antidecuplet states is inconsistent in the large N_c limit [10]. In contrast, many theories consistently predicted a stable heavy pentaquark state. The pentaquark with one heavy antiquark was first studied in Refs. [11,12] in a quark model with color spin interaction. Then it has been studied in quark models with flavor spin interaction [13] and Skyrme models [14,15], and with the recent experiments, attracted renewed interest [16–18], some of which were

motivated by the diquark-diquark [19] and diquark-triquark [20] picture. Such states also appear naturally in a coupled channel approach [21], and in the combined large N_c and heavy quark limit of QCD [22]. If the heavy pentaquark state is stable against strong decay, as was predicted in the D meson bound soliton models [14], it could only be observed from the weak decay of the virtual D meson. From a constituent quark model picture based on the color spin interaction [23], one expects a strong diquark correlation, from which one could have a stable diquark-diquark-antiquark [19] or diquark-triquark [12] structure. The question is whether such a strong diquark structure will survive other nonperturbative QCD dynamics in a multi-quark environment and produce a stable pentaquark state. Such questions are being intensively pursued in quark model approaches [24–26]. In particular, an important question at hand is whether the net attraction from the diquark correlations in the pentaquark configuration is stronger than that from the corresponding diquark and additional quark-antiquark correlation present when the pentaquark separates into a nucleon and a meson state. Since the correlation is inversely proportional to the constituent quark masses involved, the attraction is expected to be more effective for a pentaquark state with heavy antiquark. Another nonperturbative approach that can be used to answer this question is the QCD sum rule method.

There have been several QCD sum rule calculations for the light pentaquark states [27–33]. The application to the heavy pentaquarks was performed by two of us in a previous work [34], where we used a pentaquark current composed of two diquarks and an antiquark, and found the sum rule to be consistent with a stable positive-parity pentaquark state. A similar approach has been applied to the sum rules for $D_s(2317)$ [35]. In this work, we extend the previous QCD sum rule calculation to investigate the anticharmed pentaquark state with and without strangeness using two different currents for each case. We find a convergent operator product expansion (OPE) only for the nonstrange heavy pentaquark sum rule obtained with

*Electronic address: ysarac@metu.edu.tr

†Electronic address: hungchon@postech.ac.kr

‡Electronic address: suhoun@phya.yonsei.ac.kr

an interpolating field composed of two diquarks and one anticharm quark that has been previously used by us [34]. The stability of a nonstrange heavy pentaquark is consistent with the result based on the quark model with flavor spin interaction [25]. We then refine the convergent sum rule by explicitly including the DN two-particle irreducible contribution. The importance of subtracting out such a two-particle irreducible contribution has been emphasized in Refs. [36–38] for the light pentaquark state. In fact, estimating the contribution from the lowest two-particle irreducible contribution is equally important in lattice gauge theory calculations [39,40] to isolate the signal for the pentaquark state from the low-lying continuum state. We find that for the nonstrange heavy pentaquark sum rule, including the DN continuum contribution tends to shift the position of the pentaquark state downwards. Given the negative experimental signatures of the charmed pentaquark states above the threshold, the present result suggests that the anticharmed pentaquark states might be bound as was predicted in D meson bound soliton models.

This paper is organized as follows. In Sec. II, we introduce the interpolating field for the Θ_c and discuss the dispersion relations that we will be using. Section III gives the phenomenological side and Sec. IV gives the OPE side. The QCD sum rules for Θ_c and their analysis are given in Sec. V.

II. QCD SUM RULES

A. Interpolating field for Θ_c

Let us introduce the following two interpolating fields for Θ_c :

$$\begin{aligned}\Theta_{c1} &= \epsilon^{abc}(u_a^T C \gamma_\mu u_b) \gamma_5 \gamma_\mu d_c (\bar{c}_d i \gamma_5 d_d), \\ \Theta_{c2} &= \epsilon^{abk}(\epsilon^{aef} u_e^T C \gamma_5 d_f)(\epsilon^{bgh} u_g^T C d_h) C \bar{c}_k^T.\end{aligned}\quad (1)$$

Here the Roman indices a, b, \dots are color indices, C denotes charge conjugation, and T transpose. Note that Θ_{c1} is composed of a nucleon current (*proton*) and a pseudoscalar current (D), while Θ_{c2} is composed of a diquark-diquark-antiquark and has been investigated in a previous work [34].

For the charmed pentaquark with strangeness, we consider the following two possible currents:

$$\begin{aligned}\Theta_{cs1} &= \epsilon^{abk}(\epsilon^{aef} u_e^T C s_f)(\epsilon^{bgh} u_g^T C d_h) C \bar{c}_k^T, \\ \Theta_{cs2} &= \epsilon^{abk}(\epsilon^{aef} u_e^T C \gamma_5 s_f)(\epsilon^{bgh} u_g^T C d_h) C \bar{c}_k^T.\end{aligned}\quad (2)$$

Here, instead of choosing Θ_{cs1} as a direct product of a nucleon and a D_s or a hyperon and a D meson current as in Θ_{c1} , we choose it to well represent a state having two diquark structures with the same scalar quantum number but with different flavor. Such configuration allows all the five constituent quarks to be in the s -wave states, which will have the lowest orbital energy and consequently could be the dominant ground state configuration [18]. Moreover,

as we will see, Θ_{c1} couples dominantly to the nucleon and D meson state, suggesting that currents composed of a nucleon and a meson current are not suitable for investigating the properties of the pentaquark state.

Under parity transformation $q'(x') = \gamma_0 q(x)$, the Θ_c currents transform as

$$\begin{aligned}\Theta'_{c1} &= -\gamma_0 \Theta_{c1}, & \Theta'_{c2} &= \gamma_0 \Theta_{c2}, \\ \Theta'_{cs1} &= -\gamma_0 \Theta_{cs1}, & \Theta'_{cs2} &= \gamma_0 \Theta_{cs2}.\end{aligned}\quad (3)$$

B. Dispersion relation

The first types of QCD sum rules for the heavy pentaquarks that we will be using are constructed from the following time ordered correlation function:

$$\begin{aligned}\Pi_T(q) &= i \int d^4x e^{iq \cdot x} \langle 0 | T[\Theta_c(x), \bar{\Theta}_c(0)] | 0 \rangle \\ &\equiv \Pi_1(q^2) + \not{q} \Pi_q(q^2),\end{aligned}\quad (4)$$

where Θ_c can be any of the currents in Eq. (1) or in Eq. (2), and Π_q, Π_1 are called the chiral-even and chiral-odd parts, respectively. As can be seen in Eq. (3), the currents are not eigenstates of the parity transformation and can couple to both positive- and negative-parity states. The spectral densities calculated from the OPE of Eq. (4) are matched to that obtained from the phenomenological assumption in the Borel-weighted dispersion integral,

$$\int_{m_c^2}^{S_0} dq^2 e^{-q^2/M^2} W(q^2) \frac{1}{\pi} \text{Im}[\Pi_i^{\text{phen}}(q^2) - \Pi_i^{\text{ope}}(q^2)] = 0, \quad (i = 1, q), \quad (5)$$

where M^2 is the Borel mass. Here, higher resonance contributions are subtracted according to the QCD duality assumption, which introduces the continuum threshold S_0 . We have also introduced an additional weight function $W(q^2)$ for later use.

In this work, we will also work with the ‘‘old-fashioned’’ correlation function, which is defined as [29]

$$\Pi_T(q) = i \int d^4x e^{iq \cdot x} \langle 0 | \theta(x^0) \Theta_c(x) \bar{\Theta}_c(0) | 0 \rangle. \quad (6)$$

This type of correlation function has been used in projecting out positive- and negative-parity nucleon states [41]. We then divide the imaginary part into the following two parts, which are defined only for $q_0 > 0$,

$$\frac{1}{\pi} \text{Im} \Pi(q_0) = A(q_0) \gamma^0 + B(q_0). \quad (7)$$

One should note that these can be identified with the

imaginary part calculated from Eq. (4),

$$A(q_0) = \frac{1}{\pi} \text{Im} \Pi_q(q_0) q_0, \quad B(q_0) = \frac{1}{\pi} \text{Im} \Pi_1(q_0), \quad (8)$$

for $q_0 > 0$.

Now, depending on the parity of the current Θ_c in Eq. (3), one can extract the positive- or negative-parity physical state only by either adding or subtracting A and B . That is, the spectral density for the positive- and negative-parity physical states will be as follows:

$$\rho^\pm(q_0) = \begin{cases} A(q_0) \mp B(q_0) & \text{for } \Theta_{c1}, \Theta_{cs1}, \\ A(q_0) \pm B(q_0) & \text{for } \Theta_{c2}, \Theta_{cs2}. \end{cases} \quad (9)$$

The sum rules are then obtained by again matching the corresponding spectral density from the OPE and phenomenological side,

$$\int_0^\infty dq_0 e^{-q_0^2/M^2} [\rho_{\text{phen}}^\pm(q_0) - \rho_{\text{ope}}^\pm(q_0)] = 0. \quad (10)$$

III. PHENOMENOLOGICAL SIDE

A. $\Theta_{c1}, \Theta_{cs1}$

For the Θ_{c1} current, the interpolating field couples to a positive-parity state as

$$\langle 0 | \Theta_{c1}(x) | \Theta_c(\mathbf{p}): P = + \rangle = \lambda_{+,c1} \gamma_5 U_\Theta(\mathbf{p}) e^{-ip \cdot x}, \quad (11)$$

and to a negative-parity state as

$$\langle 0 | \Theta_{c1}(x) | \Theta_c(\mathbf{p}): P = - \rangle = \lambda_{-,c1} U_\Theta(\mathbf{p}) e^{-ip \cdot x}. \quad (12)$$

$$\begin{aligned} \frac{1}{\pi} \text{Im} \Pi_{T,c1}^{\text{pole}}(q) &= \not{q} |\lambda_{\pm,c1}|^2 \delta(q^2 - m_\Theta^2) \mp m_\Theta |\lambda_{\pm,c1}|^2 \delta(q^2 - m_\Theta^2), \\ \frac{1}{\pi} \text{Im} \Pi_{T,c1}^{DN}(q) &= \not{q} |\lambda_{DN,c1}|^2 \frac{q^2 + m_N^2 - m_D^2}{32\pi^2 q^4} \sqrt{q^4 - 2q^2(m_N^2 + m_D^2) + (m_N^2 - m_D^2)^2} + |\lambda_{DN,c1}|^2 \frac{2m_N}{32\pi^2 q^2} \\ &\quad \times \sqrt{q^4 - 2q^2(m_N^2 + m_D^2) + (m_N^2 - m_D^2)^2}. \end{aligned} \quad (15)$$

We notice that the chiral-odd part has opposite sign depending on the parity while the chiral-even part has a positive-definite coefficient.

B. $\Theta_{c2}, \Theta_{cs2}$

As can be seen in Eq. (3), Θ_{c2} transforms differently compared to Θ_{c1} under parity. Thus, the couplings to the interpolating field are

$$\begin{aligned} \langle 0 | \Theta_{c2}(x) | \Theta_c(\mathbf{p}): P = + \rangle &= \lambda_{+,c2} U_\Theta(\mathbf{p}) e^{-ip \cdot x}, \\ \langle 0 | \Theta_{c2}(x) | \Theta_c(\mathbf{p}): P = - \rangle &= \lambda_{-,c2} \gamma_5 U_\Theta(\mathbf{p}) e^{-ip \cdot x}. \end{aligned} \quad (16)$$

Similarly, the coupling to the DN continuum state changes as follows:

Here $\lambda_{\pm,c1}$ denotes the coupling strength between the interpolating field and the physical state with the specified parity. Similar relations will hold for Θ_{cs1} . Using these, we obtain the phenomenological side of Eq. (4) separated into chiral-even (Π_q) and -odd (Π_1) parts, which are defined to be the parts proportional to \not{q} and 1, respectively.

As was first pointed out in Ref. [36], the correlation function can also couple to the DN continuum state, whose threshold could be lower than the expected Θ_c mass. Its phenomenological contribution can be estimated by using

$$\langle 0 | \Theta_{c1} | DN(\mathbf{p}) \rangle = i \lambda_{DN,c1} U_N(\mathbf{p}). \quad (13)$$

Combining these two contributions, we find

$$\begin{aligned} \Pi_{T,c1}^{\text{phen}}(q) &= -|\lambda_{\pm,c1}|^2 \frac{\not{q} \mp m_\Theta}{q^2 - m_\Theta^2} - i |\lambda_{DN,c1}|^2 \\ &\quad \times \int d^4 p \frac{(\not{p} + m_N)}{p^2 - m_N^2} \frac{1}{(p - q)^2 - m_D^2} + \dots, \end{aligned} \quad (14)$$

where the minus (plus) sign in front of m_Θ is for positive (negative) parity. The dots denote higher resonance contributions that should be parametrized according to QCD duality. It should be noted however that higher resonances with different parities contribute differently to the chiral-even and chiral-odd parts [42]. Thus, Π_q^{phen} and Π_1^{phen} constitute separate sum rules. For Θ_{cs1} , the D meson should be replaced by the D_s meson.

The corresponding spectral density for the pole and DN contributions are given, respectively, by

$$\langle 0 | \Theta_{c2} | DN(\mathbf{p}) \rangle = \lambda_{DN,c2} \gamma_5 U_N(\mathbf{p}). \quad (17)$$

Combining these changes, we find

$$\begin{aligned} \Pi_{T,c2}^{\text{phen}}(q) &= -|\lambda_{\pm,c2}|^2 \frac{\not{q} \pm m_\Theta}{q^2 - m_\Theta^2} \\ &\quad + i |\lambda_{DN,c2}|^2 \int d^4 p \frac{\gamma_5 (\not{p} + m_N) \gamma_5}{p^2 - m_N^2} \\ &\quad \times \frac{1}{(p - q)^2 - m_D^2} + \dots. \end{aligned} \quad (18)$$

Consequently, the spectral densities are

$$\begin{aligned} \frac{1}{\pi} \text{Im}\Pi_{T,c2}^{\text{pole}}(q) &= \not{q} |\lambda_{\pm,c2}|^2 \delta(q^2 - m_{\Theta}^2) \pm m_{\Theta} |\lambda_{\pm,c2}|^2 \delta(q^2 - m_{\Theta}^2), \\ \frac{1}{\pi} \text{Im}\Pi_{T,c2}^{DN}(q) &= \not{q} |\lambda_{DN,c2}|^2 \frac{q^2 + m_N^2 - m_D^2}{32\pi^2 q^4} \sqrt{q^4 - 2q^2(m_N^2 + m_D^2) + (m_N^2 - m_D^2)^2} - |\lambda_{DN,c2}|^2 \frac{2m_N}{32\pi^2 q^2} \\ &\quad \times \sqrt{q^4 - 2q^2(m_N^2 + m_D^2) + (m_N^2 - m_D^2)^2}. \end{aligned} \quad (19)$$

C. Phenomenological side

The final form for the phenomenological side to be used in Eq. (10) can be obtained from combining Eq. (15) or Eq. (19) according to Eq. (9), both of which are given in the following form:

$$\begin{aligned} \rho_{\text{phen}}^{\pm}(q_0) &= |\lambda_{\pm}|^2 \delta(q_0 - m_{\Theta}) + \theta(\sqrt{s_0} - q_0) \rho_{DN}^{\pm}(q_0) \\ &\quad + \theta(q_0 - \sqrt{s_0}) \rho_{\text{cont}}^{\pm}(q_0), \end{aligned} \quad (20)$$

where the usual duality assumption has been used to represent the higher resonance contribution above the continuum threshold $\sqrt{s_0}$; i.e., $\rho_{\text{cont}}^{\pm}(q_0) = \rho_{\text{ope}}^{\pm}(q_0)$. The spectral density for the two-particle irreducible part is given by

$$\begin{aligned} \rho_{DN,c1}^{\pm}(q_0) &= \frac{|\lambda_{DN,c1}|^2}{32\pi^2} \sqrt{(q_0 - m_D)^2 - m_N^2} \\ &\quad \times \sqrt{(q_0 + m_D)^2 - m_N^2} \frac{(q_0 \pm m_N)^2 - m_D^2}{q_0^3}, \end{aligned} \quad (21)$$

$$\begin{aligned} \rho_{DN,c2}^{\pm}(q_0) &= \frac{|\lambda_{DN,c2}|^2}{32\pi^2} \sqrt{(q_0 - m_D)^2 - m_N^2} \\ &\quad \times \sqrt{(q_0 + m_D)^2 - m_N^2} \frac{(q_0 \mp m_N)^2 - m_D^2}{q_0^3}. \end{aligned} \quad (22)$$

We substitute the above into the Borel transformed dispersion relation in Eq. (10).

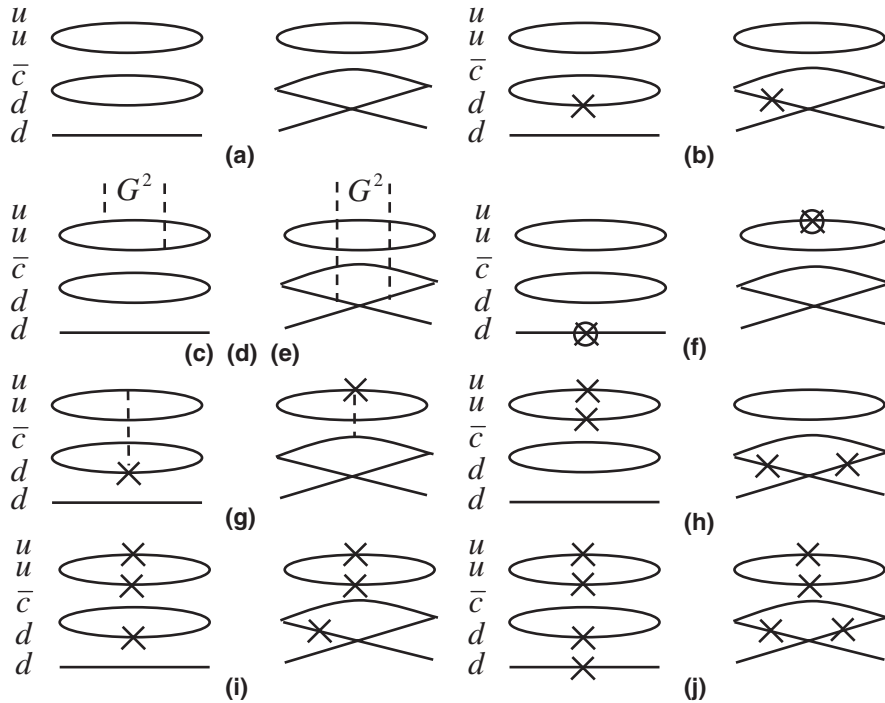


FIG. 1. Schematic OPE diagrams for the current Θ_{c1} in Eq. (1). Each label corresponds to that in Eq. (24). The solid lines denote quark (or anticharm quark) propagators and the dashed lines are for the gluon. The crosses denote the quark condensate, and the crosses with circles represent the mixed quark-gluon condensates. (c) represents diagrams proportional to a gluon condensate with gluons lines attached to the light quarks only, (d) represents those where the gluons are attached to the heavy quarks only, while (e) represents those where one gluon is attached to the heavy quark and the other to a light quark in all possible ways. (f) and (g) represent all diagrams that contain the quark-gluon condensate.

IV. OPE SIDE

A. Θ_{c1}

Here, we present the result for Θ_{c1} . To keep the charm-quark mass finite, we use the momentum-space expression for the charm-quark propagators. For the light-quark part of the correlation function, we calculate in the coordinate space, which is then Fourier transformed to the momentum space in D dimension. The resulting light-quark part is

combined with the charm-quark part before it is dimensionally regularized at $D = 4$.

Our OPE is given by

$$\begin{aligned} \Pi^{\text{ope},c1}(q) = & \Pi^{(a)} + \Pi^{(b)} + \Pi^{(c)} + \Pi^{(d)} + \Pi^{(e)} \\ & + \Pi^{(f)} + \Pi^{(g)} + \Pi^{(h)} + \Pi^{(i)} + \Pi^{(j)}, \end{aligned} \quad (23)$$

where the superscript indicates each diagram in Fig. 1. The imaginary part of each diagram is calculated as

$$\begin{aligned} \frac{1}{\pi} \text{Im}\Pi^{(a)}(q^2) &= \frac{11}{516!2^{13}\pi^8} \int_0^\Lambda du \frac{1}{(1-u)^5} \{ \not{q}[-36u(1-u)[-L(u)]^5 + 120q^2u^2(1-u)^2[-L(u)]^4 + m_c72[-L(u)]^5 \}, \\ \frac{1}{\pi} \text{Im}\Pi^{(b)}(q^2) &= \frac{5\langle\bar{q}q\rangle}{4!4!2^9\pi^8} \int_0^\Lambda du \frac{1}{(1-u)^3} \{ \not{q}16m_cu[-L(u)]^3 + 8q^2u(1-u)[-L(u)]^3 - [-L(u)]^4 \}, \\ \frac{1}{\pi} \text{Im}\Pi^{(c)}(q^2) &= -\frac{11\langle\frac{\alpha_s}{\pi}G^2\rangle}{3 \cdot 4!2^{14}\pi^6} \int_0^\Lambda du \frac{1}{(1-u)^3} \left\{ \not{q}[-3u(1-u)[-L(u)]^3 + 6q^2u^2(1-u)^2[-L(u)]^2 \right. \\ &\quad \left. - \frac{8}{11}(1-u)[-L(u)]^3 + \frac{12}{11}m_c[-L(u)]^3 \right\}, \\ \frac{1}{\pi} \text{Im}\Pi^{(d)}(q^2) &= \frac{11\langle\frac{\alpha_s}{\pi}G^2\rangle}{3!6!2^{12}\pi^6} \int_0^\Lambda du \frac{u^3}{(1-u)^5} \left\{ \not{q}m_c^2[-3u(1-u)[-L(u)]^2 + 4q^2u^2(1-u)^2[-L(u)] \right. \\ &\quad \left. + m_c \left[\frac{4}{11}[-L(u)]^3 + \frac{6}{11}q^2(1-u)^2[-L(u)]^2 \right] \right\}, \\ \frac{1}{\pi} \text{Im}\Pi^{(e)}(q^2) &= \frac{\langle\frac{\alpha_s}{\pi}G^2\rangle}{4!5!3 \cdot 2^{10}\pi^6} \int_0^\Lambda du \frac{u}{(1-u)^4} \{ \not{q}[(96u(1-u) + 5(1-u))[-L(u)]^3 - 192q^2u^2(1-u)^2[-L(u)]^2 \\ &\quad + 90m_c[-L(u)]^3 \}, \\ \frac{1}{\pi} \text{Im}\Pi^{(f)}(q^2) &= \frac{5\langle\bar{q}g\sigma \cdot Gq\rangle}{3!3!2^{11}\pi^6} \int_0^\Lambda du \frac{1}{(1-u)^2} \{ 12\not{q}m_cu[-L(u)]^2 - [-L(u)]^3 + 6q^2u(1-u)[-L(u)]^2 \}, \\ \frac{1}{\pi} \text{Im}\Pi^{(g)}(q^2) &= \frac{\langle\bar{q}g\sigma \cdot Gq\rangle}{3!4!2^{10}\pi^6} \int_0^\Lambda du \frac{1}{(1-u)^3} \left\{ \not{q}m_c[12u(1-u)[-L(u)]^2 - 60u^2[-L(u)]^2 - 12(1-u)[-L(u)]^3 \right. \\ &\quad \left. + 72q^2u(1-u)^2[-L(u)]^2 - \frac{u}{2}[-L(u)]^3 + 3q^2u^2(1-u)[-L(u)]^2 \right\}, \\ \frac{1}{\pi} \text{Im}\Pi^{(h)}(q^2) &= \frac{\langle\bar{q}q\rangle^2}{9 \cdot 2^9\pi^4} \int_0^\Lambda du \frac{1}{(1-u)^2} \{ \not{q}[12u(1-u)[-L(u)]^2 - 16q^2u^2(1-u)^2[-L(u)] \\ &\quad + 3(1-u)[-L(u)]^2 + 27m_c[-L(u)]^2 \}, \\ \frac{1}{\pi} \text{Im}\Pi^{(i)}(q^2) &= \frac{5\langle\bar{q}q\rangle^3}{9 \cdot 2^4\pi^2} \int_0^\Lambda du \{ -\not{q}m_cu + [-L(u)] - 2q^2u(1-u) \}, \\ \frac{1}{\pi} \text{Im}\Pi^{(j)}(q^2) &= \frac{\langle\bar{q}q\rangle^4}{216} (-\not{q} + 22m_c)\delta(q^2 - m_c^2). \end{aligned} \quad (24)$$

Here the upper limit of the integrations is given by $\Lambda = 1 - m_c^2/q^2$ and $L(u) = q^2u(1-u) - m_c^2u$. Our OPE calculation has been performed up to dimension 12 here. Up to dimension 5, we include all the gluonic contributions represented by the gluon condensate and the quark-gluon mixed condensate. Beyond the dimension 5, we have included only tree-graph contributions which are expected to be important among higher dimensional operators. Other

diagrams containing gluon components are expected to be suppressed by the small QCD coupling. Therefore, the higher order tree graphs, which are the higher order quark condensates, will be able to give us an estimate on how big the typical higher order corrections should be beyond dimension 5. The integrations can be done analytically but we skip the messy analytic expressions. For the charm-quark propagators with two gluons attached, we

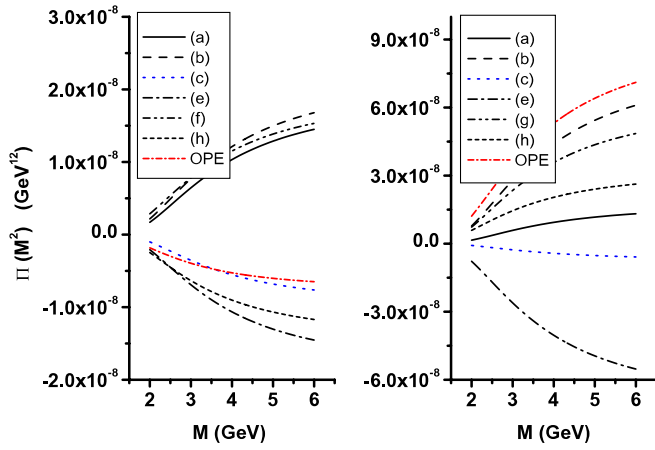


FIG. 2 (color online). OPE as defined in Eq. (25) for the current Θ_{c1} and $S_0 = (3.3 \text{ GeV})^2$. The left (right) figure is for the positive- (negative-) parity case. The solid line (a) represents the perturbative contribution. The line specified as OPE represents the sum of the power corrections only. (c) represents the gluon condensates. Other labels represent the contribution from each term in Eq. (24). Here we plot only a few selected terms in the OPE.

use the momentum-space expressions given in Ref. [43]. The Wilson coefficients for light-quark condensates come from $\langle \bar{q}q \rangle^n$, where $n = 2, 3, 4$. This is in contrast with the OPE for Θ_{c2} , where the Wilson coefficient are nonzero only for $n = 4$.

The first important question to ask in the OPE is whether it is sensibly converging as an asymptotic expansion. For that, we choose to plot the Borel transformed OPE appearing in Eq. (10) after subtracting out the continuum contribution,

$$\Pi^{(j)}(M^2) = \int_0^\infty dq_0 e^{-q_0^2/M^2} [\rho_{\text{ope}}^{\pm,(j)}(q_0) - \rho_{\text{cont}}^{\pm,(j)}(q_0)] = 0. \quad (25)$$

Here $j = a, b, c, \dots$ denotes each contribution in the OPE in Eq. (24) after adding according to the rules in Eq. (9).

We use the following QCD parameters in our sum rules [29,44]:

$$\begin{aligned} m_s &= 0.12 \text{ GeV}, & m_c &= 1.26 \text{ GeV}, \\ \left\langle \frac{\alpha_s}{\pi} G^2 \right\rangle &= (0.33 \text{ GeV})^4, & \langle G^3 \rangle &= 0.045 \text{ GeV}^6, \\ \langle \bar{q}q \rangle &= -(0.23 \text{ GeV})^3, & \langle \bar{s}s \rangle &= 0.8 \langle \bar{q}q \rangle, \\ \langle \bar{q}g\sigma \cdot Gq \rangle &= (0.8 \text{ GeV}^2) \times \langle \bar{q}q \rangle, \\ \langle \bar{s}g\sigma \cdot Gs \rangle &= (0.8 \text{ GeV}^2) \times \langle \bar{s}s \rangle. \end{aligned} \quad (26)$$

Figure 2 represents the OPE as defined in Eq. (25) with the imaginary part in Eq. (24). One notes that for the negative-parity case, the perturbative contribution is only a small fraction of the OPE, and hence does not converge. For the positive-parity case, the power corrections alternate in signs, and the gluon condensate, which represents the light diquark correlation, is only a small correction to the power correction. Hence, such structure would hardly couple to a pentaquark state, and it is meaningless to perform a detailed QCD sum rule analysis. We present the result with the continuum threshold $S_0 = (3.3 \text{ GeV})^2$. This value is chosen in the range $\sqrt{S_0} = 3.2\text{--}3.6 \text{ GeV}$, which has been used to analyze the anticharmed-pentaquark sum rule in Ref. [34]. However changing S_0 does not change the relative strength of each contribution and hence the conclusion of this section. We will therefore analyze the subsequent OPE with the same threshold.

B. Θ_{c2}

The OPE for Θ_{c2} is given in Ref. [34]. Here, we rewrite the result for completeness,

$$\begin{aligned} \frac{1}{\pi} \text{Im}\Pi^{(a)}(q^2) &= -\frac{1}{5 \cdot 5!2^{12}\pi^8} \int_0^\Lambda du \frac{1}{(1-u)^5} \{\not{q}(1-u) + m_c\} [-L(u)]^5, \\ \frac{1}{\pi} \text{Im}\Pi^{(b)}(q^2) &= -\frac{1}{3!3!2^{10}\pi^6} \left\langle \frac{\alpha_s}{\pi} G^2 \right\rangle \int_0^\Lambda du \frac{1}{(1-u)^3} \{\not{q}(1-u) + m_c\} [-L(u)]^3, \\ \frac{1}{\pi} \text{Im}\Pi^{(c)}(q^2) &= -\frac{1}{54} \langle \bar{q}q \rangle^4 (\not{q} + m_c) \delta(q^2 - m_c^2), \\ \frac{1}{\pi} \text{Im}\Pi^{(d)}(q^2) &= -\frac{1}{5!3!3 \cdot 2^{10}\pi^6} \left\langle \frac{\alpha_s}{\pi} G^2 \right\rangle \int_0^\Lambda du \frac{u^3}{(1-u)^5} \{3m_c^2 \not{q}(1-u) + m_c(1-u)(3-5u)q^2 + 2um_c^3\} [-L(u)]^2, \\ \frac{1}{\pi} \text{Im}\Pi^{(e)}(q^2) &= -\frac{\langle G^3 \rangle}{5!4!2^{13}\pi^8} \int_0^\Lambda du \frac{u}{(1-u)} \left\{ \not{q} \left[q^2 \left(\frac{5u}{2} - 1 \right) (1-u) - m_c^2 \left(\frac{3u}{2} + 7 \right) \right] \right. \\ &\quad \left. + 6m_c q^2 (2u-1) - 2m_c^3 \frac{3u+1}{1-u} \right\} [-L(u)]. \end{aligned} \quad (27)$$

The diagrams corresponding to every term above, denoted by the superscripts (a)–(e), can be found in Ref. [34].

Figure 3 represents the OPE as defined in Eq. (25) with the imaginary part in Eq. (27). As can be seen from the left figure, the OPE without the perturbative contribution is dominated by the gluon condensate coming from the light diquarks. This suggests that the diquark correlation is the dominant interaction among the quarks and heavy antiquark in the positive-parity channel. Moreover, the perturbative contribution is larger than the sum of the power corrections denoted as ‘‘OPE’’ in the figure. Therefore, the pentaquark could couple strongly to this current and a detailed QCD sum rule analysis is sensible. The situation changes for the negative channel, where the power corrections have alternating signs, and hence becomes less reliable.

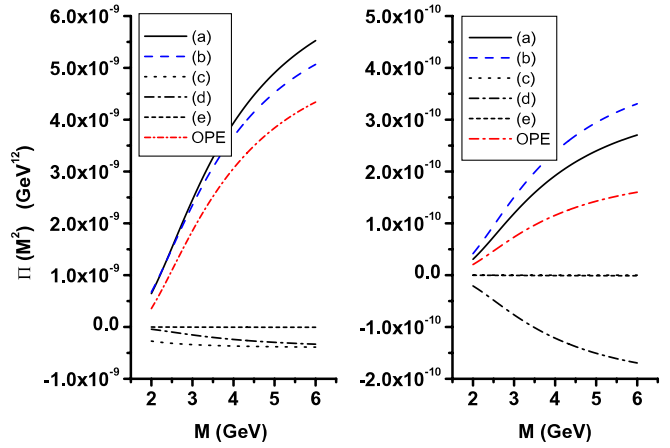


FIG. 3 (color online). A similar figure as Fig. 2 for the current Θ_{c2} . Here each label represents the contribution from each term in Eq. (27). The gluon condensates (b) are the dominant power correction in the positive-parity channel (left figure).

C. Θ_{cs1}

The OPE for this current is given as follows:

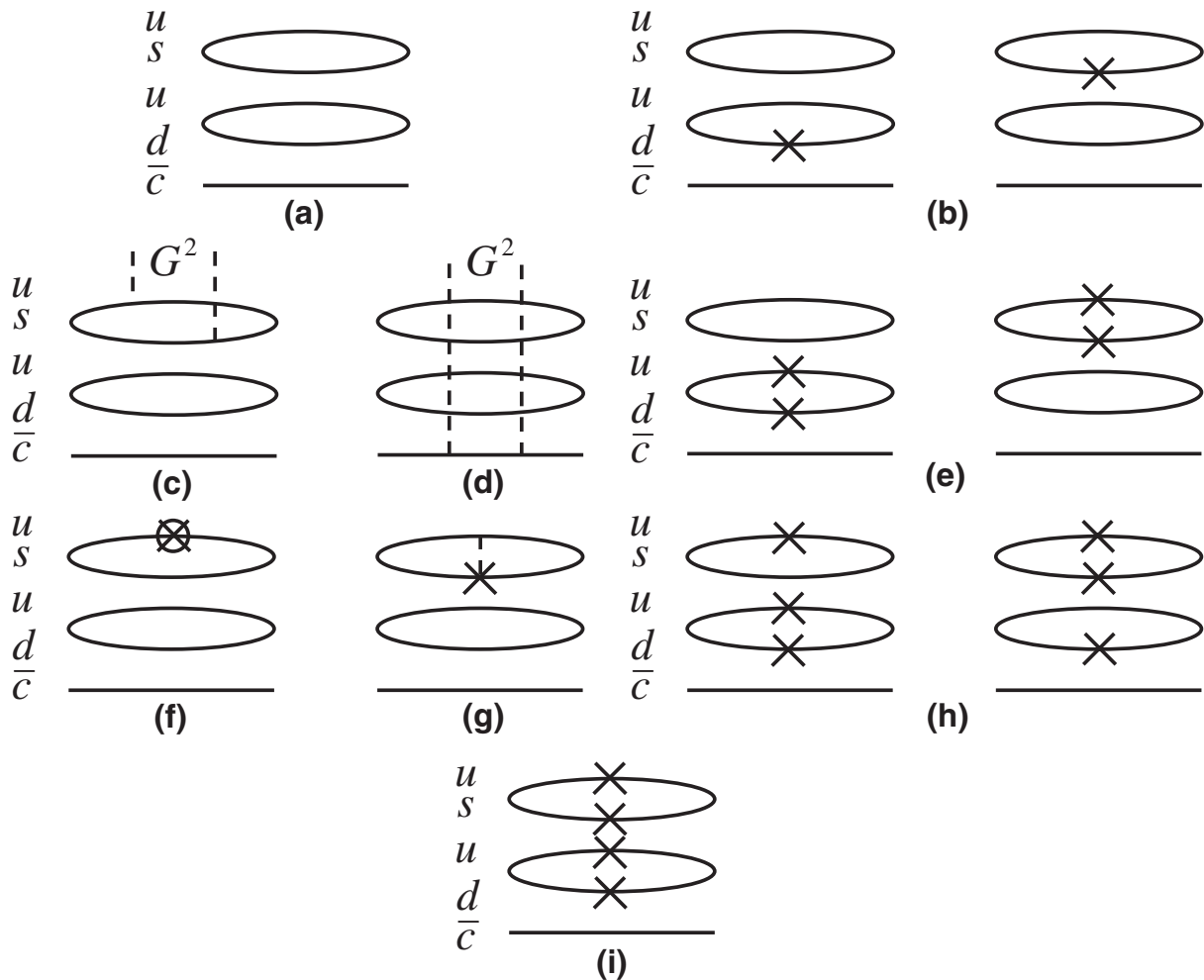


FIG. 4. Schematic OPE diagrams for the currents Θ_{cs1} in Eq. (28) and Θ_{cs2} in Eq. (29). Each label corresponds to that in Eq. (28) or Eq. (29). All the other notations in this figure are the same as Fig. 1.

$$\begin{aligned}
 \frac{1}{\pi} \text{Im}\Pi^{(a)}(q^2) &= \frac{1}{5 \cdot 5!2^{12}\pi^8} \int_0^\Lambda du \frac{1}{(1-u)^5} \{\not{d}(u-1) - m_c\}[-L(u)]^5, \\
 \frac{1}{\pi} \text{Im}\Pi^{(b)}(q^2) &= \frac{m_s(2\langle\bar{q}q\rangle + \langle\bar{s}s\rangle)}{3!3!2^8\pi^6} \int_0^\Lambda du \frac{1}{(1-u)^3} \{\not{d}(u-1) - m_c\}[-L(u)]^3, \\
 \frac{1}{\pi} \text{Im}\Pi^{(c)}(q^2) &= \frac{\langle\frac{\alpha_s}{\pi}G^2\rangle}{3!3!2^{10}\pi^6} \int_0^\Lambda du \frac{1}{(1-u)^3} \{\not{d}(u-1) - mc\}[-L(u)]^3, \\
 \frac{1}{\pi} \text{Im}\Pi^{(d)}(q^2) &= -\frac{\langle\frac{\alpha_s}{\pi}G^2\rangle}{3 \cdot 3!5!2^{10}\pi^6} \int_0^\Lambda du \frac{u^3}{(1-u)^5} \{\not{d}3m_c^2(1-u) + m_c(1-u)(3-5u)q^2 + 2um_c^3\}[-L(u)]^2, \\
 \frac{1}{\pi} \text{Im}\Pi^{(e)}(q^2) &= \frac{\langle\bar{q}q\rangle^2 + \langle\bar{q}q\rangle\langle\bar{s}s\rangle}{3 \cdot 2^7\pi^4} \int_0^\Lambda du \frac{1}{(1-u)^2} \{\not{d}(u-1) - m_c\}[-L(u)]^2, \\
 \frac{1}{\pi} \text{Im}\Pi^{(f)}(q^2) &= \frac{m_s\langle\bar{q}D^2q\rangle}{2^{10}\pi^6} \int_0^\Lambda du \frac{1}{(1-u)^2} \{\not{d}(u-1) - m_c\}[-L(u)]^2, \\
 \frac{1}{\pi} \text{Im}\Pi^{(g)}(q^2) &= \frac{m_s\langle\bar{s}g\sigma \cdot Gs\rangle}{3 \cdot 2^{11}\pi^6} \int_0^\Lambda du \frac{1}{(1-u)^2} \{\not{d}(u-1) - m_c\}[-L(u)]^2, \\
 \frac{1}{\pi} \text{Im}\Pi^{(h)}(q^2) &= \frac{m_s(2\langle\bar{q}q\rangle^3 + \langle\bar{q}q\rangle^2\langle\bar{s}s\rangle)}{9 \cdot 2^4\pi^2} \int_0^\Lambda du \{\not{d}(u-1) - m_c\}, \\
 \frac{1}{\pi} \text{Im}\Pi^{(i)}(q^2) &= \frac{\langle\bar{q}q\rangle^3\langle\bar{s}s\rangle}{54} (\not{d} + m_c)\delta(q^2 - m_c^2).
 \end{aligned} \tag{28}$$

Note here again that the superscripts correspond to the diagrams shown in Fig. 4. The dimension-5 condensate involving D^2 is related to the quark-gluon condensate via $\langle\bar{q}D^2q\rangle = \langle\bar{q}g\sigma \cdot Gq\rangle/2$. A similar relation holds for the corresponding strange-quark condensate. The correction to this relation is proportional to the square of the quark mass which should be very small even for the strange quark. Figure 5 represents the OPE as defined in Eq. (25) with the imaginary part in Eq. (28). We have included only a few terms in the OPE to show how each term contributes differently to the sum rule. As can be seen from the figure,

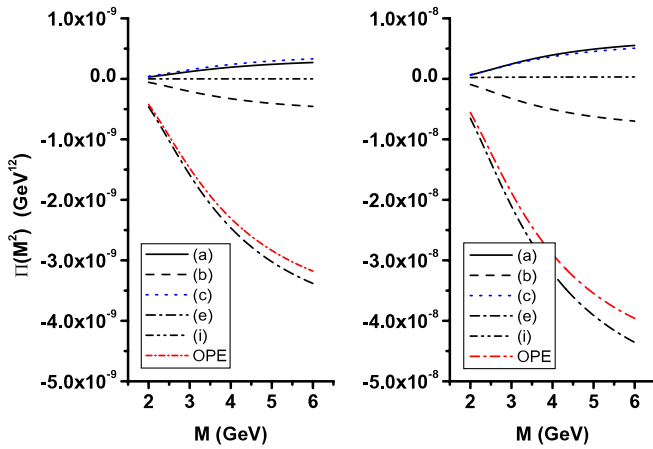


FIG. 5 (color online). A similar figure as Fig. 2 for the current Θ_{cs1} with $S_0 = (3.3 \text{ GeV})^2$. Here each label represents a contribution from each term in Eq. (28).

the lines denoted as OPE, which is a sum of the power corrections only, are much larger than the perturbative contribution. Moreover, the gluon condensate from diquarks is only a small fraction of the large higher order correction. This suggests that the OPE is not convergent and it is very unlikely that the diquark correlation will remain an important mechanism in this configuration.

D. Θ_{cs2}

The OPE for this current is given as follows:

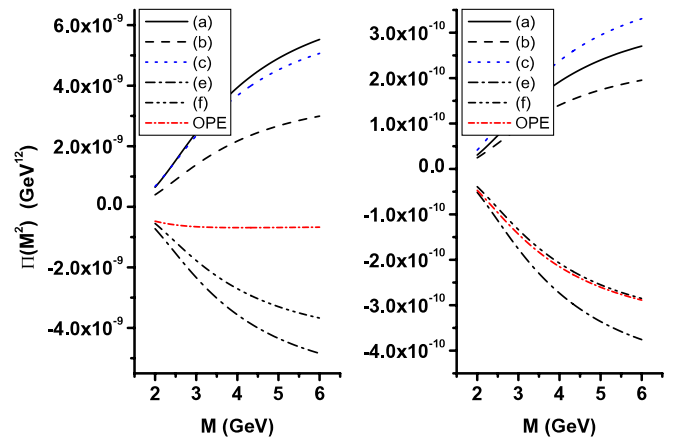


FIG. 6 (color online). A similar figure as Fig. 2 for the current Θ_{cs2} with $S_0 = (3.3 \text{ GeV})^2$. Here each label represents each term in Eq. (29).

$$\begin{aligned}
 \frac{1}{\pi} \text{Im}\Pi^{(a)}(q^2) &= \frac{1}{5 \cdot 5!2^{12}\pi^8} \int_0^\Lambda du \frac{1}{(1-u)^5} \{\not{d}(u-1) - m_c\} [-L(u)]^5, \\
 \frac{1}{\pi} \text{Im}\Pi^{(b)}(q^2) &= \frac{m_s(-2\langle\bar{q}q\rangle + \langle\bar{s}s\rangle)}{3!3!2^8\pi^6} \int_0^\Lambda du \frac{1}{(1-u)^3} \{\not{d}(u-1) - m_c\} [-L(u)]^3, \\
 \frac{1}{\pi} \text{Im}\Pi^{(c)}(q^2) &= \frac{\langle\frac{\alpha_s}{\pi}G^2\rangle}{3!3!2^{10}\pi^6} \int_0^\Lambda du \frac{1}{(1-u)^3} \{\not{d}(u-1) - m_c\} [-L(u)]^3, \\
 \frac{1}{\pi} \text{Im}\Pi^{(d)}(q^2) &= -\frac{\langle\frac{\alpha_s}{\pi}G^2\rangle}{3 \cdot 3!5!2^{10}\pi^6} \int_0^\Lambda du \frac{u^3}{(1-u)^5} \{\not{d}3m_c^2(1-u) + m_c(1-u)(3-5u)q^2 + 2um^3\} [-L(u)]^2, \\
 \frac{1}{\pi} \text{Im}\Pi^{(e)}(q^2) &= \frac{(\langle\bar{q}q\rangle^2 - \langle\bar{q}q\rangle\langle\bar{s}s\rangle)}{3 \cdot 2^7\pi^4} \int_0^\Lambda du \frac{1}{(1-u)^2} \{\not{d}(u-1) - m_c\} [-L(u)]^2, \\
 \frac{1}{\pi} \text{Im}\Pi^{(f)}(q^2) &= \frac{-m_s\langle\bar{q}D^2q\rangle}{2^{10}\pi^6} \int_0^\Lambda du \frac{1}{(1-u)^2} \{\not{d}(u-1) - m_c\} [-L(u)]^2, \\
 \frac{1}{\pi} \text{Im}\Pi^{(g)}(q^2) &= \frac{m_s\langle\bar{s}g\sigma \cdot Gs\rangle}{3 \cdot 2^{11}\pi^6} \int_0^\Lambda du \frac{1}{(1-u)^2} \{\not{d}(u-1) - m_c\} [-L(u)]^2, \\
 \frac{1}{\pi} \text{Im}\Pi^{(h)}(q^2) &= \frac{m_s(-2\langle\bar{q}q\rangle^3 + \langle\bar{q}q\rangle^2\langle\bar{s}s\rangle)}{9 \cdot 2^4\pi^2} \int_0^\Lambda du \{\not{d}(u-1) - m_c\}, \\
 \frac{1}{\pi} \text{Im}\Pi^{(i)}(q^2) &= \frac{-\langle\bar{q}q\rangle^3\langle\bar{s}s\rangle}{54} (\not{d} + m_c)\delta(q^2 - m_c^2). \tag{29}
 \end{aligned}$$

Again note that the OPE diagram for each label is shown in Fig. 4. Figure 6 represents the OPE as defined in Eq. (25) with the imaginary part in Eq. (29). Again, we have included only a few terms in the OPE to show a general trend of each contribution. For the negative-parity case, the OPE has large contributions with alternating signs. The situation is better for the positive-parity case, but again, the power corrections alternate in signs.

From all the previous analysis on the OPE for the charmed pentaquark with and without strangeness, we find that the ones without strangeness with a diquark structure are most reliable and are dominated by a gluon condensate coming from the diquark correlation. It is interesting to note that this result is consistent with the Skyrme model calculation which predicts a bound state of pentaquarks in the nonstrange sector [15]. In the following, we will perform a more detailed analysis with the stable structure well represented by the interpolating current Θ_{c2} .

V. QCD SUM RULES AND ANALYSIS

A. The couplings to the DN continuum, λ_{DN}

As discussed before, it is important to subtract out the contribution from the DN continuum. For that, one needs to know the coupling strength λ_{DN} . Here we determine this for the currents without strange quarks, $\lambda_{DN,c2}$. In the case of Θ^+ (1540) [37], the soft-kaon theorem was used to convert the external kaon state, corresponding to the D meson states in Eqs. (13) and (17), to a commutation relation of the operator and the corresponding axial charge. The strength of the resulting five-quark operator with an external nucleon state was then obtained from a separate

nucleon sum rule analysis with the same five-quark nucleon current. However, applying the soft D meson limit will obviously not work in the present case.

Instead, we determine the coupling strength directly from the sum rule method. To do that, we eliminate the contribution from the low-lying pole by introducing the additional weight $W(q^2) = q^2 - m_\Theta^2$ in Eq. (5). We will take $m_\Theta = 3$ GeV and confirmed that changing it by ± 200 MeV will have less than 5% effect on the λ_{DN} value. This way of eliminating a certain pole is sometimes used in QCD sum rules [45,46]. Then, substituting the corresponding imaginary parts, we find

$$|\lambda_{DN}|^2 = \frac{\int_{m_c^2}^{S_0} dq^2 e^{-q^2/M^2} (q^2 - m_\Theta^2) \frac{1}{\pi} \text{Im}\Pi_i^{\text{ope}}(q^2)}{\int_{(m_N+m_D)^2}^{S_0} dq^2 e^{-q^2/M^2} (q^2 - m_\Theta^2) \frac{1}{\pi} \text{Im}\Pi_i^{DN}(q^2)}, \tag{30}$$

($i = 1, q$),

where the $i = 1, q$ in $\text{Im}\Pi$ represent the part proportional to 1 or \not{d} in the respective imaginary part, and $\text{Im}\Pi^{DN}$ is the spectral density in Eq. (15) or in Eq. (19) without the $|\lambda_{DN}|^2$.

Figure 7 shows the plot of Eq. (30). The two dotted (solid) lines represent boundary curves with the least Borel mass dependence for the λ_{DN} from the 1 (q) sum rules. λ_{DN} should not only be independent of the Borel mass but also independent of the sum rule from which it is obtained. However, the results coming from either the $i = q$ or the $i = 1$ sum rule differ slightly. Inspecting the OPE, one finds that the contributions from higher dimensional operators are consecutively suppressed for the $i = q$ sum rule, while that is not so for the $i = 1$ sum rule.

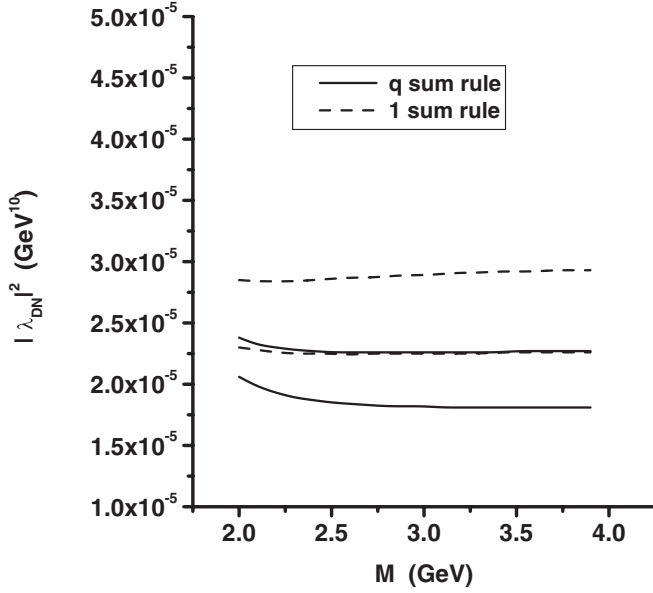


FIG. 7. The $|\lambda_{DN,c2}|^2$ from the sum rule for $i = q$ (solid lines) and $i = 1$ (dashed lines). The upper (lower) solid or dashed lines in this case are for $S_0 = (3.8 \text{ GeV})^2$ [$S_0 = (3.7 \text{ GeV})^2$].

Therefore, the value from the former sum rule should be more reliable. Nonetheless, to allow for all variations, we will choose the following range for the $|\lambda_{DN}|^2$ values:

$$2 \times 10^{-5} \text{ GeV}^{10} < |\lambda_{DN,c2}|^2 < 3 \times 10^{-5} \text{ GeV}^{10}. \quad (31)$$

Similar attempts to determine $\lambda_{DN,c1}$ give vastly different values from either $i = q$ or $i = 1$ sum rules. This reflects the nonconvergence of OPE from which one cannot expect a consistent result.

B. Parity

We will now concentrate on the sum rule obtained from Θ_{c2} . Using the dispersion relation in Eq. (10) and the spectral density in Eq. (20), one finds the following sum rule:

$$|\lambda_{\pm,c2}|^2 e^{-m_{\Theta_{\pm}}^2/M^2} = \int_0^{\sqrt{s_0}} dq_0 e^{-q_0^2/M^2} [\rho_{\text{ope}}^{\pm}(q_0) - \rho_{DN}^{\pm}(q_0)]. \quad (32)$$

As can be seen from Fig. 8, the left-hand side of Eq. (32) is positive for the positive-parity case. For $|\lambda_{DN,c2}|^2 = 0$ (the solid lines), we have chosen the continuum threshold $S_0^{1/2}$ to be 3.4 and 3.3 GeV, which gives the most stable pentaquark mass as we will show in the next subsection. A similar method was used to obtain the continuum thresholds when $|\lambda_{DN,c2}|^2 \neq 0$. However, Fig. 9 shows that the corresponding sum rule is negative for the negative-parity case, suggesting that there cannot be any negative-parity state. This result also confirms the nonconvergence of the OPE for the negative-parity case, from which a consistent result cannot be obtained. This can also be expected from

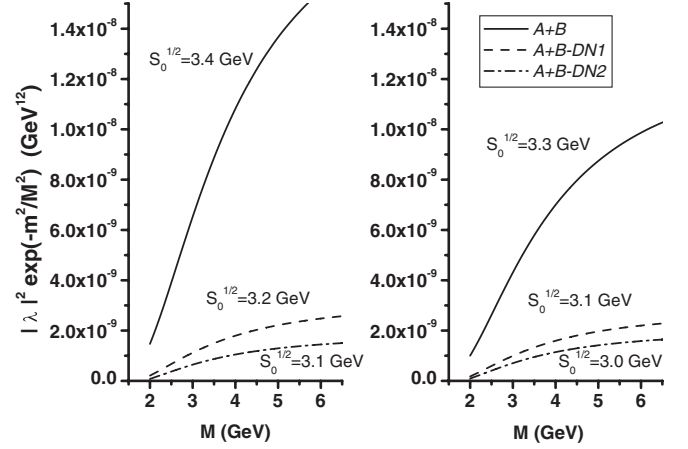


FIG. 8. The left figure shows the left-hand side of Eq. (32) using Θ_{c2} for the positive-parity case with $|\lambda_{DN,c2}|^2 = 2 \times 10^{-5} \text{ GeV}^{10}$ (dashed line) and $|\lambda_{DN,c2}|^2 = 3 \times 10^{-5} \text{ GeV}^{10}$ (dot-dashed line). The solid line is when there is no DN continuum, $|\lambda_{DN,c2}|^2 = 0$. The right figure is obtained with different threshold parameters. See Eq. (8) for A and B .

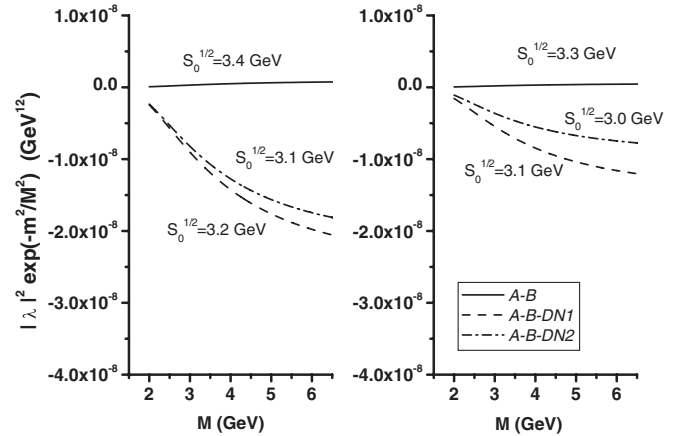


FIG. 9. The left figure shows the left-hand side of Eq. (32) using Θ_{c2} for the negative-parity case with $|\lambda_{DN,c2}|^2 = 2 \times 10^{-5} \text{ GeV}^{10}$ (dashed line) and $|\lambda_{DN,c2}|^2 = 3 \times 10^{-5} \text{ GeV}^{10}$ (dot-dashed line). The solid line is when there is no DN continuum. The right figure is obtained with different threshold parameters.

the constituent quark picture. The two diquarks in the Θ_{c2} current have opposite parities and, when they are combined with the antiquark, the configuration should be dominated by the positive-parity part in the nonrelativistic limit.

C. Mass

The sum rule for the Θ_c mass is obtained by taking the derivative of Eq. (32) with respect to $1/M^2$. The solid and dashed lines in Fig. 10 represent the mass for two different λ_{DN} values. The threshold parameters were obtained to give the most stable mass within the Borel window plotted. One notes that for the inclusion of the coupling to the DN

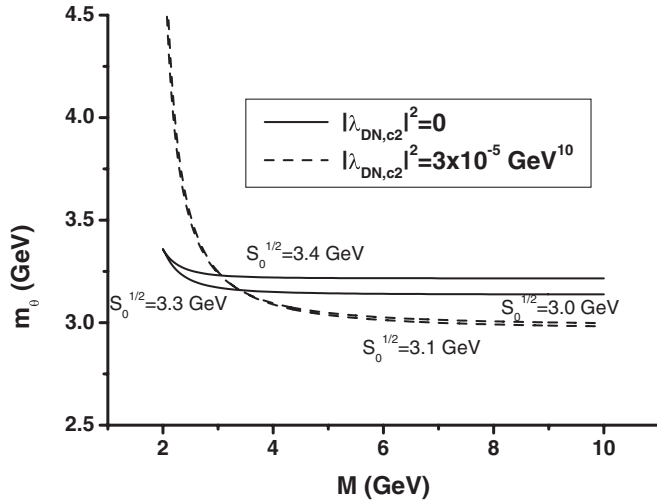


FIG. 10. The mass obtained by taking the square root of the inverse ratio between the left-hand side of Eq. (32) and its derivative with respect to M^2 using Θ_{c2} .

continuum states, the mass reduces to smaller values to below 3 GeV. The curve with $\lambda_{DN,c2} = 2 \times 10^{-5} \text{ GeV}^{10}$ lies between the solid and dashed lines in Fig. 10. This suggests the possibility that the heavy pentaquark might actually be bound, namely, lies below the DN threshold. This is consistent with the constituent quark model picture, where one expects the diquark correlation to be more dominant than that of the quark-antiquark correlation as the participating antiquark becomes heavy. However, if this

was the case, its existence can only be measured through its weak decay.

VI. SUMMARY

We have performed the OPE and QCD sum rule analysis for heavy pentaquark with and without strangeness with two different currents each. We find that the OPE is convergent only for the nonstrange pentaquark with diquark structure. The OPE for this structure is dominated by the gluon condensate coming from the diquark, which non-perturbatively represents their strong correlation. We find that the heavy pentaquark without strangeness has a positive parity as reported earlier [34] and that its mass lies below 3 GeV, when the DN irreducible contribution is explicitly included in the phenomenological side of the sum rule. The picture that we described here does not work so well in the light pentaquark Θ^+ , as the OPEs are highly divergent [47] as can be seen in the picture of the OPE in the original sum rule paper for the light pentaquark state [29].

ACKNOWLEDGMENTS

We are grateful to A. Hosaka and Fl. Stancu for fruitful discussions. The work of S.H.L. was supported by the Korea Research Foundation under Grant No. C00116. The work of Y.S. was supported by the Scientific and Technological Research Council of Turkey.

- [1] T. Nakano *et al.* (LEPS Collaboration), Phys. Rev. Lett. **91**, 012002 (2003).
- [2] S. Stepanyan *et al.* (CLAS Collaboration), Phys. Rev. Lett. **91**, 252001 (2003); J. Barth *et al.* (SAPHIR Collaboration), Phys. Lett. B **572**, 127 (2003); V. V. Barmin *et al.* (DIANA Collaboration), Yad. Fiz. **66**, 1763 (2003) [Phys. At. Nucl. **66**, 1715 (2003)]; V. Kubarovsky and S. Stepanyan (CLAS Collaboration), AIP Conf. Proc. **698**, 543 (2004); A. E. Asratyan, A. G. Dolgolenko, and M. A. Kubantsev, Yad. Fiz. **67**, 704 (2004) [Phys. At. Nucl. **67**, 682 (2004)]; V. Kubarovsky *et al.* (CLAS Collaboration), Phys. Rev. Lett. **92**, 032001 (2004); A. Airapetian *et al.* (HERMES Collaboration), Phys. Lett. B **585**, 213 (2004); A. Aleev *et al.* (SVD Collaboration), hep-ex/0401024; M. Abdel-Bary *et al.* (COSY-TOF Collaboration), Phys. Lett. B **595**, 127 (2004); S. Chekanov *et al.* (ZEUS Collaboration), Phys. Lett. B **591**, 7 (2004); Y. Oh, H. Kim, and S. H. Lee, Phys. Rev. D **69**, 014009 (2004); **69**, 094009 (2004); **69**, 074016 (2004); Nucl. Phys. A **745**, 129 (2004); S. H. Lee, H. Kim, and Y. Oh, J. Korean Phys. Soc. **46**, 774 (2005); Y. Oh and H. Kim, Phys. Rev. D **70**, 094022 (2004).
- [3] E. Smith, "Review on JLAB results," talk given at Hadron 05, <http://www.cbpf.br/hadron05/>
- [4] For a review on the present status of pentaquarks, see K. H. Hicks, Prog. Part. Nucl. Phys. **55**, 647 (2005).
- [5] A. Aktas *et al.* (H1 Collaboration), Phys. Lett. B **588**, 17 (2004).
- [6] D. O. Litvintsev *et al.* (CDF Collaboration), Nucl. Phys. B, Proc. Suppl. **142**, 374 (2005).
- [7] U. Karshon *et al.* (ZEUS Collaboration), hep-ex/0410029.
- [8] J. M. Link *et al.* (FOCUS Collaboration), Phys. Lett. B **622**, 229 (2005).
- [9] D. Diakonov, V. Petrov, and M. V. Polyakov, Z. Phys. A **359**, 305 (1997).
- [10] T. D. Cohen, Phys. Lett. B **581**, 175 (2004).
- [11] C. Gignoux, B. Silvestre-Brac, and J. M. Richard, Phys. Lett. B **193**, 323 (1987).
- [12] H. J. Lipkin, Phys. Lett. B **195**, 484 (1987).
- [13] Fl. Stancu, Phys. Rev. D **58**, 111501 (1998); M. Genovese, J.-M. Richard, Fl. Stancu, and S. Pepin, Phys. Lett. B **425**, 171 (1998).
- [14] D. O. Riska and N. N. Scoccola, Phys. Lett. B **299**, 338 (1993).

- [15] Y. Oh, B.-Y. Park, and D.-P. Min, Phys. Lett. B **331**, 362 (1994); Phys. Rev. D **50**, 3350 (1994); Y. Oh and B.-Y. Park, Phys. Rev. D **51**, 5016 (1995); Y. s. Oh and B. Y. Park, Z. Phys. A **359**, 83 (1997).
- [16] K. Cheung, Phys. Rev. D **69**, 094029 (2004); T.E. Browder, I.R. Klebanov, and D.R. Marlow, Phys. Lett. B **587**, 62 (2004); M.A. Nowak, M. Praszalowicz, M. Sadzikowski, and J. Wasiluk, Phys. Rev. D **70**, 031503 (2004); H.Y. Cheng, C.K. Chua, and C.W. Hwang, Phys. Rev. D **70**, 034007 (2004); M.E. Wessling, Phys. Lett. B **603**, 152 (2004); **618**, 269(E) (2005); F. Stancu, Int. J. Mod. Phys. A **20**, 1797 (2005); K. Maltman, Int. J. Mod. Phys. A **20**, 1977 (2005).
- [17] D. Pirjol and C. Schat, Phys. Rev. D **71**, 036004 (2005).
- [18] I. W. Stewart, M. E. Wessling, and M. B. Wise, Phys. Lett. B **590**, 185 (2004).
- [19] R.L. Jaffe and F. Wilczek, Phys. Rev. Lett. **91**, 232003 (2003).
- [20] M. Karliner and H.J. Lipkin, Phys. Lett. B **575**, 249 (2003).
- [21] J. Hofmann and M. F. M. Lutz, hep-ph/0507071.
- [22] T.D. Cohen, P.M. Hohler, and R. F. Lebed, Phys. Rev. D **72**, 074010 (2005).
- [23] R.L. Jaffe, Phys. Rev. Lett. **38**, 195 (1977); **38**, 617(E) (1977).
- [24] E. Hiyama, M. Kamimura, A. Hosaka, H. Toki, and M. Yahiro, hep-ph/0507105 [Phys. Lett. B (to be published)].
- [25] F. Stancu, AIP Conf. Proc. **775**, 32 (2005).
- [26] K. Maltman, Phys. Lett. B **604**, 175 (2004).
- [27] S.L. Zhu, Phys. Rev. Lett. **91**, 232002 (2003).
- [28] R.D. Matheus, F. S. Navarra, M. Nielsen, R. Rodrigues da Silva, and S. H. Lee, Phys. Lett. B **578**, 323 (2004).
- [29] J. Sugiyama, T. Doi, and M. Oka, Phys. Lett. B **581**, 167 (2004).
- [30] M. Eidemuller, Phys. Lett. B **597**, 314 (2004).
- [31] H.J. Lee, N. I. Kochelev, and V. Vento, Phys. Lett. B **610**, 50 (2005); H.J. Lee, N. I. Kochelev, and V. Vento, hep-ph/0506250.
- [32] M. Eidemuller, F.S. Navarra, M. Nielsen, and R. Rodrigues da Silva, Phys. Rev. D **72**, 034003 (2005).
- [33] R.D. Matheus, F.S. Navarra, M. Nielsen, and R.R. da Silva, Phys. Lett. B **602**, 185 (2004).
- [34] H. Kim, S.H. Lee, and Y. Oh, Phys. Lett. B **595**, 293 (2004).
- [35] H. Kim and Y. Oh, Phys. Rev. D **72**, 074012 (2005); M. E. Bracco, A. Lozea, R. D. Matheus, F. S. Navarra, and M. Nielsen, Phys. Lett. B **624**, 217 (2005).
- [36] Y. Kondo, O. Morimatsu, and T. Nishikawa, Phys. Lett. B **611**, 93 (2005).
- [37] S.H. Lee, H. Kim, and Y. Kwon, Phys. Lett. B **609**, 252 (2005).
- [38] Y. Kwon, A. Hosaka, and S. H. Lee, hep-ph/0505040.
- [39] S. Sasaki, Phys. Rev. Lett. **93**, 152001 (2004).
- [40] F. Csikor, Z. Fodor, S. D. Katz, and T. G. Kovacs, J. High Energy Phys. **11** (2003) 070.
- [41] D. Jido, N. Kodama, and M. Oka, Phys. Rev. D **54**, 4532 (1996).
- [42] X.M. Jin and J. Tang, Phys. Rev. D **56**, 515 (1997).
- [43] L.J. Reinders, H. Rubinstein, and S. Yazaki, Phys. Rep. **127**, 1 (1985).
- [44] M. A. Shifman, A. I. Vainshtein, and V. I. Zakharov, Nucl. Phys. **B147**, 385 (1979).
- [45] X. m. Jin, Phys. Rev. D **55**, 1693 (1997).
- [46] H. Kim and M. Oka, Nucl. Phys. **A720**, 368 (2003).
- [47] R. D. Matheus and S. Narison, hep-ph/0412063